Report 8, 1993

DISTRIBUTED PARAMETER MODELS FOR THE SVARTSENGI GEOTHERMAL FIELD, SW-ICELAND AND THE YANGBAJING GEOTHERMAL FIELD, TIBET, CHINA

Hu Baigeng,
UNU Geothermal Training Programme,
Orkustofnun - National Energy Authority,
Grensasvegur 9,
108 Reykjavik,
ICELAND

Permanent address:
Thermal Engineering Department,
Tsinghua University,
Beijing, 100084,
P.R. CHINA

ABSTRACT

This report describes distributed parameter models of two geothermal reservoirs. The basic equations of the problem are derived and the reservoir behaviour of two different geothermal fields is analyzed.

The first field is the Svartsengi geothermal field in southwest Iceland. For this well-developed geothermal field, a lot of data collection and analysis has been carried out during the last seventeen years. The calibration in this report is to match the water level drawdown measurement in several wells. The obtained reservoir parameters confirm the former research work in this field.

The second field is the Yangbajing geothermal field in Tibet, China. Similar to the Svartsengi geothermal field, it is also liquid-dominated system with a two-phase zone on the top. Despite insufficient time-dependent production data and continuous water level measurement in observation wells, the obtained reservoir parameters were used to predict the response of the reservoir in the future. If production is increased from 200 to 550 kg/s, the future water level drawdown is predicted to increase quickly. Therefore, the influence of two different reinjection schemes has also been taken into account, including the subsequent temperature decline due to reinjection.

TABLE OF CONTENTS

LIST OF FIGURES

LIST OF TABLES

1. INTRODUCTION

In recent years, the use of geothermal reservoir modelling has been much developed. Numerous quantitative models for different geothermal fields are available. The main scope of this work is the calibration of reservoir parameters and the prediction of future response of the reservoir due to different production rates and reinjection. The calibration and prediction processes were carried out by using the AQUA programme package developed by Vatnaskil Consulting Engineers.

The author of this report had the opportunity to be a United Nations University Fellow specializing in reservoir engineering in Reykjavik, Iceland for six months in 1993. The Geothermal Training Programme started with a two-month series of lectures on various subjects concerning aspects of exploration, production and utilization of geothermal energy all over the world, especially in Iceland. After this, the UNU Fellows went on an excursion around the high and low temperature geothermal fields in Iceland. The last two and a half months were spent on simulation work and preparation of this report. The author was carefully guided by his supervisors Dr. Snorri Pall Kjaran and Mr. Sigurdur Larus Holm throughout this period.

The first part of the work is about the Svartsengi geothermal field in SW-Iceland. The second part of the work is about the Yangbajing geothermal field in Tibet, China.

2. DISTRIBUTED PARAMETER MODELS

A number of different models for modelling the behaviour of geothermal reservoirs are currently available to reservoir engineers. These models vary widely in complexity and cost of application. Geothermal systems are generally very complicated, exhibiting such features as fracture dominated flow, phase change, chemical reactions, and thermal effects. After a plausible conceptual model of the field is developed, one must choose a numerical model which can realistically evaluate the performance of the geothermal reservoir and reliably predict its future behaviour (Bodvarsson et al., 1986). The AQUA programme package developed by Vatnaskil Consulting Engineers (1990) is a general mathematical model that can be used to simulate a geothermal reservoir in as much detail as desired. The basic equations solved in distributed parameter models are mass and energy conservation equations.

The AQUA programme package solves ground-water flow and transport equations using the Galerkin finite element method. The following differential equation is the basis for the mathematical model:

$$a\frac{\partial u}{\partial t} + b_i\frac{\partial u}{\partial x_i} + \frac{\partial}{\partial x_i}(e_{ij}\frac{\partial u}{\partial x_j}) + fu + g = 0 \qquad (1)$$

The model is two-dimensional, and indices i and j indicate the x and y coordinate axes.

The system requirements for AQUA are as follows: IBM PC/XT/AT or compatible, MS-DOS version 2 or later, 553K of free memory, EGA graphics card and display, hard disk, 8087/80287/80387 co-processor, digitizer and/or mouse, graphical printer and HP-plotter.

2.1 Flow model of the AQUA programme

For a transient groundwater flow, Equation 1 is reduced to

$$a\frac{\partial u}{\partial t} + \frac{\partial}{\partial x_i}(e_{ij}\frac{\partial u}{x_j}) + fu + g = 0 \qquad (2)$$

For a confined groundwater flow in a leaky aquifer, the parameters in Equation 2 are defined as:

$$u = h;\ e_{ij} = T_{ij};\ f = 0;\ g = Q + (k/m)(h_o - h);\ a = -S.$$

By using x and y instead of the indices, Equation 2 then reads:

$$\frac{\partial}{\partial x}(T_{xx}\frac{\partial h}{\partial x}) + \frac{\partial}{\partial y}(T_{yy}\frac{\partial h}{\partial y}) + \frac{k}{m}(h_o - h) + Q = S\frac{\partial h}{\partial t} \qquad (3)$$

where

- h - *ground-water head [m];*
- T_{xx} - *transmissivity along principal axis [m^2/s];*
- T_{yy} - *transmissivity perpendicular to the principal axis [m^2/s];*
- Q - *pumping/reinjection rate [m^3/s];*
- k/m - *leakage coefficient, where k is the permeability of the semipermeable layer and m is its thickness, [m/s];*
- h_o - *head in upper aquifer [m];*
- S - *storage coefficient.*

For a long term exploitation, storage in the reservoir is controlled by compressibility of the water and the rock in terms of the elastic storage coefficient as in confined aquifers and by the delayed yield effect. In this case, the equation for the transient groundwater flow is

$$\frac{\partial}{\partial x}(T_{xx}\frac{\partial h}{\partial x})+\frac{\partial}{\partial y}(T_{yy}\frac{\partial h}{\partial y})+\frac{k}{m}(h_o-h)+Q = S\frac{\partial h}{\partial t}+\alpha\phi\int_0^t\frac{\partial h}{\partial t}e^{-\alpha(t-\tau)}d\tau \tag{4}$$

where ϕ - *effective porosity;*
$\alpha = 1/\kappa$, *and* κ *is a time constant [s].*

To obtain an expression for the numerical solution of Equation 4, the following way is used:
Step n

$$i_n = \alpha n\int_0^{t_n}\frac{\partial h}{\partial t}e^{-\alpha(t-\tau)}d\tau \tag{5}$$

and step n+1

$$i_{n+1} = \alpha n\int_0^{t_{n+1}}\frac{\partial h}{\partial t}e^{-\alpha(t_{n+1}-\tau)}d\tau \tag{6}$$

The integral can be rewritten as:

$$i_{n+1} = e^{-\alpha\Delta t}i_n+\alpha ne^{-\alpha(t_n+\Delta t)}[\frac{1}{\alpha}e^{\alpha\tau}]_{t_n}^{t_{n+1}}\frac{(h_{n+1}-h_n)}{\Delta t} \tag{7}$$

and

$$i_{n+1} = e^{-\alpha\Delta t}i_n+\frac{n}{\Delta t}(h_{n+1}-h_n)(1-e^{-\alpha\Delta t}) \tag{8}$$

Now Equation 4 can be approximated by the following numerical expression;

$$-K[\theta h_{n+1}+(1-\theta)h_n] = \frac{1}{\Delta t}M(h_{n+1}-h_n)+L[\theta i_{n+1}+(1-\theta)i_n] \tag{9}$$

where θ is equal to 1, as the classic implicit approximation.

For steady-state, Equation 1 is reduced to

$$\frac{\partial}{\partial x_i}(e_{ij}\frac{\partial u}{\partial x_j})+fu+g = 0 \tag{10}$$

where we define:
$u = h$; $e_{ij} = T_{ij}$; $f = 0$; $g = Q + \gamma$; *and*
γ = *R (infiltration rate) for an unconfined horizontal aquifer [mm/year], or*
$\gamma = (k/m)(h_o-h)$ *for a confined horizontal aquifer [m/s].*

By using x and y instead of the indices, Equation 10 then reads

$$\frac{\partial}{\partial x}(T_{xx}\frac{\partial h}{\partial x})+\frac{\partial}{\partial y}(T_{yy}\frac{\partial h}{\partial y})+Q+\gamma = 0 \tag{11}$$

In the AQUA model, the following boundary conditions are allowed:

1. **Dirichlet boundary condition**, the ground-water level, the piezometric head or the potential function is prescribed at the boundary;
2. **Von Neumann boundary condition**, the flow at the boundary is prescribed by defining source nodes at the no-flow boundary nodes;
3. **Cauchy boundary condition**, the boundary flow rate is related to both the normal derivative and the head.

2.2 Mass transport model of the AQUA programme

For the mass transport model in AQUA, the parameters in Equation 1 are defined as follows:

$$u = c;\ a = \phi b R_d;\ b_i = v_i b;\ e_{ij} = -\phi b D_{ij};\ f = \phi b R_d \lambda + \gamma + Q;\ g = -\gamma c_o - Q c_w.$$

By using x and y instead of the indices, Equation 1 then reads:

$$\frac{\partial}{\partial x}(\phi b D_{xx}\frac{\partial c}{\partial x}) + \frac{\partial}{\partial y}(\phi b D_{yy}\frac{\partial c}{\partial y}) - v_x b\frac{\partial c}{\partial x} - v_y b\frac{\partial c}{\partial y} = \phi b R_d\frac{\partial c}{\partial t} + \phi b R_d \lambda c - (c_o - c)\gamma - Q(c_w - c) \quad (12)$$

The above equation applies to a local coordinate system with each element having the main axis along the flow direction. The dispersion coefficients are defined by

$$\phi D_{xx} = a_L v^n + D_m \phi \quad (13)$$

and

$$\phi D_{yy} = a_T v^n + D_m \phi \quad (14)$$

The retardation coefficient R_d is given by

$$R_d = 1 + \beta_c \frac{(1-\phi)\varrho_s}{\phi \varrho_l} \quad (15)$$

and

$$\beta_c = K_d \varrho_l \quad (16)$$

where
- c - *solute concentration [kg/m^3];*
- c_o - *solute concentration of vertical inflow [kg/m^3];*
- c_w - *solute concentration of injected water [kg/m^3];*
- v_x, v_y - *velocity vector taken from the solution of the flow problem [m^3/s];*
- a_L - *longitudinal dispersity [m];*
- a_T - *transversal dispersity [m];*
- v - *velocity [m/s];*
- D_m - *molecular diffusivity [m^2/s];*
- ϕ - *effective porosity;*
- Q - *pumping rate [m^3/s];*
- b - *aquifer thickness [m];*
- λ - *exponential decay constant [1/s];*
- K_d - *distribution coefficient;*
- ϱ_l - *density of the liquid [kg/m^3];*

ϱ_s - *density of the porous medium [kg/m^3];*
γ - *R (infiltration rate) for unconfined horizontal aquifer [mm/year];*
γ - *(k/m)(h_o-h) for confined horizontal aquifer [m/s];*
β_c - *retardation constant.*

2.3 Heat transport model of the AQUA programme

For the heat transport model, the parameters in Equation 1 are defined as follows:

$$u = T;\ a = \phi b R_h;\ b_i = v_i b;\ e_{ij} = -bK_{ij};\ f = \gamma + Q;\ g = -\gamma T_o - QT_w$$

By using x and y instead of the indices, Equation 1 then reads

$$\frac{\partial}{\partial x}(bK_{xx}\frac{\partial T}{\partial x}) + \frac{\partial}{\partial y}(bK_{yy}\frac{\partial T}{\partial y}) - v_x b\frac{\partial T}{\partial x} - v_y b\frac{\partial T}{\partial y} = \phi b R_h\frac{\partial T}{\partial t} - (T_o - T)\gamma - (T_w - T)Q \qquad (17)$$

The above equation also applies to a local coordinate system within each element having the main axis along the flow direction.

The heat dispersion coefficients are given by:

$$K_{xx} = a_L v^n + D_h\phi \qquad (18)$$

$$K_{yy} = a_T v^n + D_h\phi \qquad (19)$$

The heat retardation coefficient R_h is given by:

$$R_h = 1 + \beta_h\frac{(1-\phi)\varrho_s}{\phi\varrho_l} \qquad (20)$$

and

$$\beta_h = \frac{C_s}{C_l} \qquad (21)$$

where T - *temperature [°C];*
T_o - *temperature of the vertical inflow [°C];*
C_l - *specific heat capacity of the liquid [kJ/kg°C];*
C_s - *specific heat capacity of the porous medium [kJ/kg°C];*
β_h - *retardation constant;*
D_h - *heat diffusivity [m^2/s].*

The other parameters are defined as previously.

For both transport models, two kinds of boundary conditions are allowed:

1. **Dirichlet boundary conditions**, the concentration or temperature is specified at the boundary.
2. **Von Neumann boundary condition**, the concentration gradient or the temperature gradient is set to zero indicating convective transport of mass or heat through the boundary.

3. THE SVARTSENGI GEOTHERMAL FIELD, SW-ICELAND

3.1 The main features of the Svartsengi geothermal field

3.1.1 Locality

The Svartsengi high-temperature reservoir is among six geothermal fields associated with an active rift zone which is the landward extension of the Mid-Atlantic ridge on the Reykjanes peninsula, southwest Iceland (Figure 1). Figure 2 shows the location of the boreholes in the Svartsengi field. The accumulated rocks are of basaltic composition but were formed in two different environments: lava flow sequences erupted from a subairial volcanoes during interglacial periods, and hyaloclastite formation erupted under ice during glacial periods (Franzson, 1983). The primary porosity and permeability at the interlayers of the sub-horizontal lava flows, as well as within the hyaloclastite formations, are considered to be relatively high.

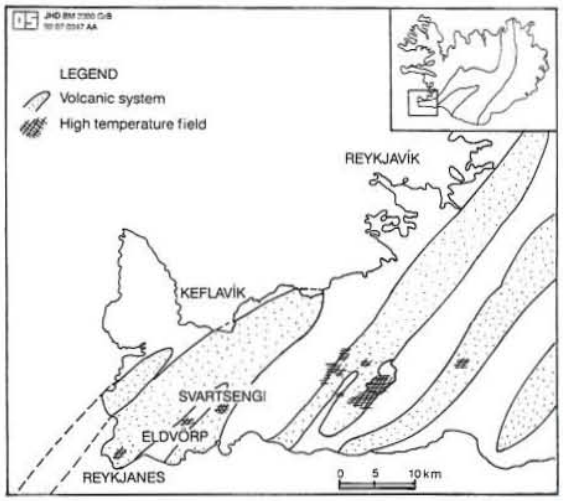

FIGURE 1: The Svartsengi field and its geological surroundings (Bjornsson and Steingrimsson, 1992)

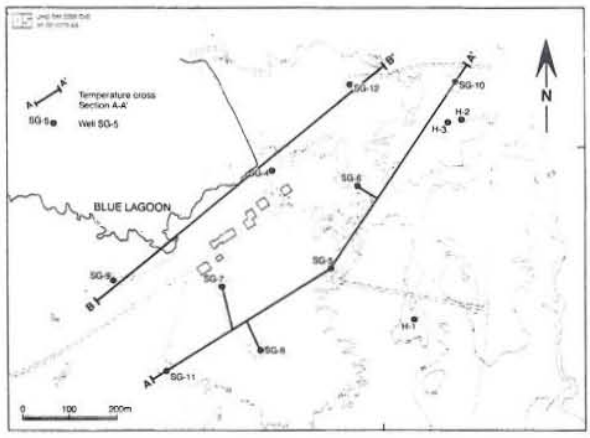

FIGURE 2: Well location in the Svartsengi field (Bjornsson and Steingrimsson, 1992)

3.1.2 The geophysical survey in the field

More than 150 Schlumberger soundings have been carried out with a maximum current electrode spacing (AB/2) of 700-1600 m in addition to numerous shallow soundings (Georgsson, 1984). The uniformity in the geology and hydrology is reflected in the horizontal resistivity layering and subtle resistivity changes within the layers. Therefore, one-dimensional inverse interpretation of the resistivity curves was, with few exceptions, found to be adequate. The NW-SE trending resistivity cross-section through the Svartsengi field (Figure 3) clearly shows the horizontal layering of the region and the low-resistivity anomaly in the Svartsengi field.

The reservoir in the Svartsengi field is characterized by a 230-240°C liquid dominated system below 600 m depth and a two-phase boiling zone extending to the surface (Bjornsson and Steingrimsson, 1992). There are 12 wells in the well field which is 1 km^2 in area extent. The reservoir fluid is a brine with salinity corresponding to about 2/3 that of sea water. The temperature distribution in cross sections A-A' and B-B' (see Figure 2 for location) are shown in Figure 4. The reservoir is furthermore assumed to be totally isolated from a warm groundwater system between 0-300 m depth.

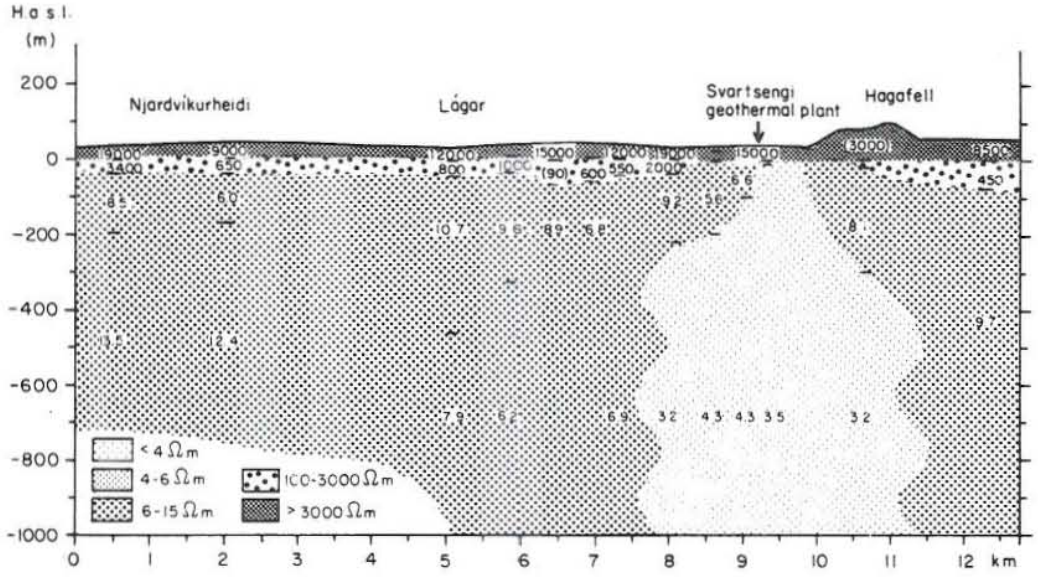

FIGURE 3: NW-SE resistivity cross-section through the Svartsengi field (Georgsson, 1984)

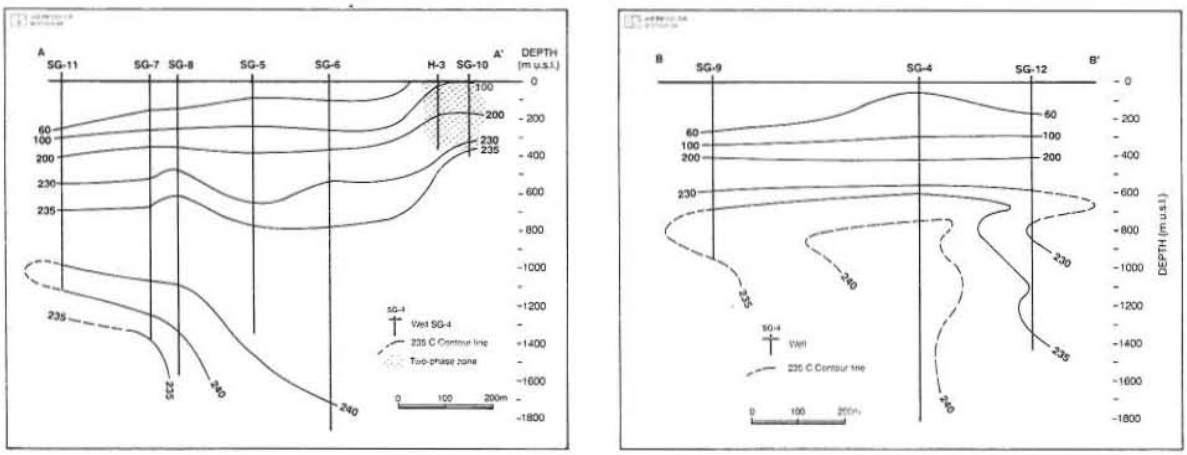

FIGURE 4: Temperature distribution in cross-section A-A' and B-B' (Bjornsson and Steingrimsson, 1992)

3.1.3 Production history and utilization

The Svartsengi high temperature field has been under exploitation since 1976. The power plant utilizes geothermal brine and steam from the Svartsengi reservoir to heat cold groundwater for district heating purposes and to generate electricity. The present capacity of the plant is 125 MW_t and 11.6 MW_e (Palmason et al., 1990). The total mass produced from the reservoir amounts to more than 80 million metric tons and the average rate of production is presently around 230 kg/s (Bjornsson et al., 1992).

3.2 Results from the calibration of the reservoir parameters

The total surface area covered by the mesh is about 1100 km^2. The model was created with 1069 nodes and 2100 elements. The boundary in the ocean was put at a sufficient distance from the production area to minimize its influence on the solution. The other boundaries are assumed to be no-flow boundaries. As for the initial state, prior to the production it was assumed that the water level in the reservoir was constant.

The transmissivity in the field varies from 4.00×10^{-4} to 0.15 m^2/s (Figure 5). The values inside the earthquake zone are relatively higher than those on the outside.

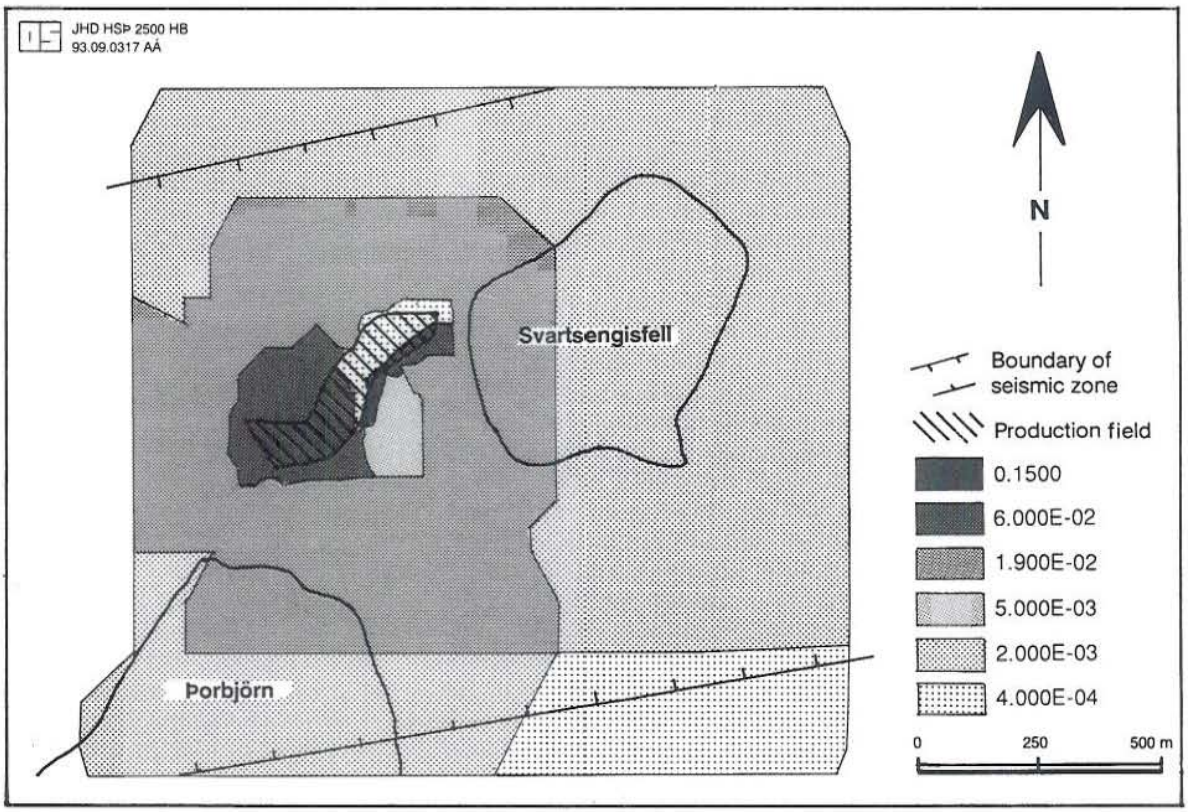

FIGURE 5: Transmissivity distribution in the Svartsengi field

The storativity coefficient and the anisotropy angle distribution in the field are shown in Figures 6 and 7. The anisotropy sqrt(T_{yy}/T_{xx}) distributions in the field from the geological survey are set at 0.477 inside the earthquake zone and at 0.158 outside. Likewise, the porosity is set at 0.05 inside the producing area and at 0.15 outside.

In the calibration process, a match between the observed and computed water level drawdown in wells 4 and 5 was achieved. The calibration results are shown in Figures 8 (well 4) and 9 (well 5).

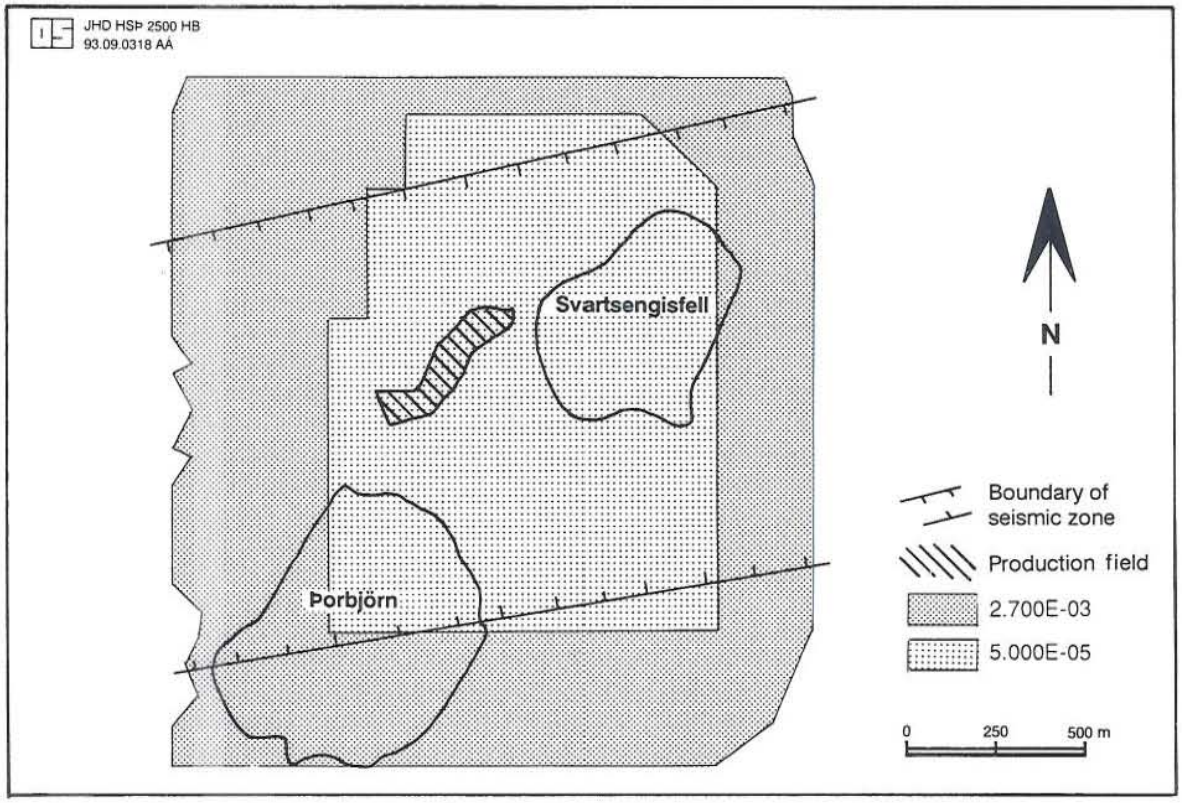

FIGURE 6: Storativity distribution in the Svartsengi field

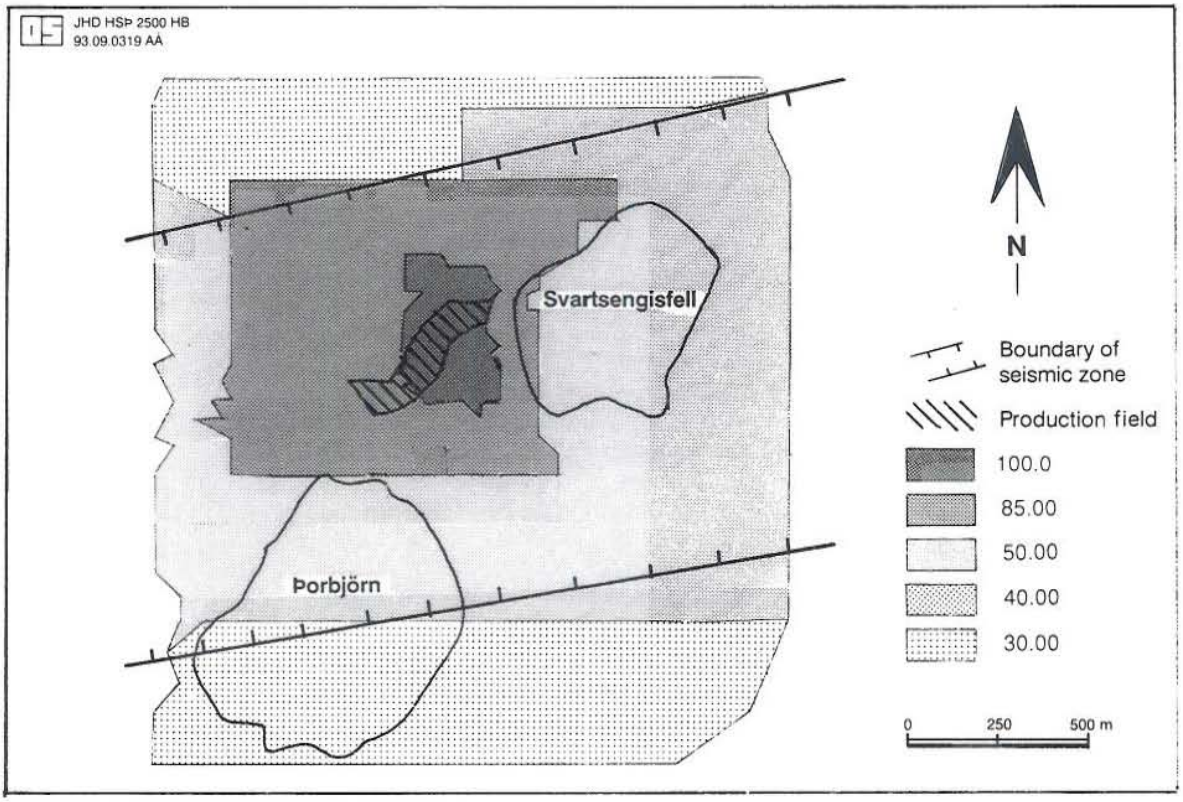

FIGURE 7: Anisotropy angle distribution in the Svartsengi field

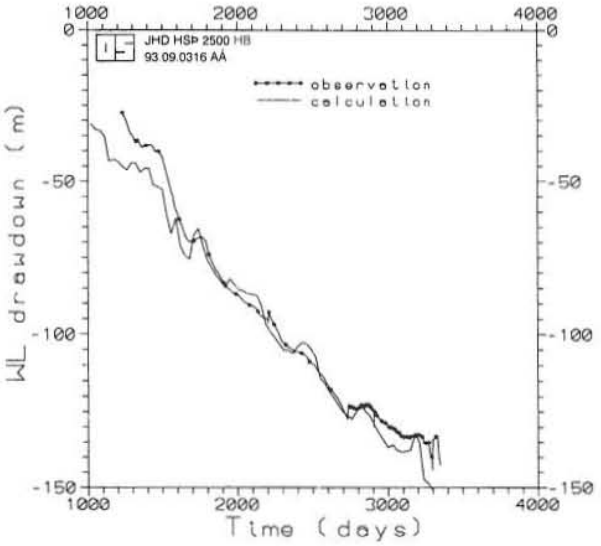

FIGURE 8: Calibration results for well 4 in the Svartsengi field

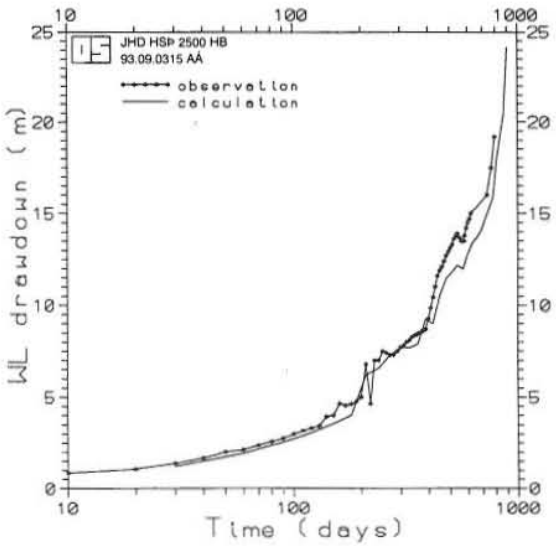

FIGURE 9: Calibration results for well 5 in the Svartsengi field

3.3 Conclusions

By using the AQUA package model, a very good fit was reached between the observation data and computed data. The detailed parameters obtained from the simulation can be applied for reasonable future prediction in the Svartsengi field. The findings on the Svartsengi geothermal field have confirmed the existence of a good connection between wells 5 and 6, and the low permeability barrier between wells 4 and 5. Moreover, the lowering of the water level due to production was too much, so reinjection is now necessary in this area.

4. THE YANGBAJING GEOTHERMAL FIELD IN TIBET, CHINA

4.1 The main features of the field

4.1.1 Locality and general outline of the field

Tibet reminds us of beautiful snow-covered mountains and warm springs. Among the springs, Yangbajing is the most famous. It is located in the Yangbajing Basin which is 90 km northwest of Lasha City, the capital of the Tibet autonomous region. The northern edge of the field is Ningqingtangula mountains at an elevation of 5500-6000 m. Tanshan mountains are in its southern boundary at about 6000 m above sea level. The basin trends gently to the northeast. It is 5 km wide and at an elevation of about 4300 m. The curving Zanbu River flows through the southern part of the field. The climate in the region is of semi-dry plateau grassland. The annual average temperature is 3.8°C. The annual average atmosphere pressure is 603.6 millibar. The annual precipitation is 453 mm and the annual evaporation is 2073 mm. Earthquakes are very common and hydrothermal activity in the basin is controlled by active tectonics. The total producing area in the Yangbajing field is about 15 km^2, 7.4 km^2 in the south and 7.6 km^2 in the north set by 40°C temperature contours.

There are three main motivations to develop geothermal energy in Tibet. The urgent requirement for energy in Lasha City and Tibet region is the first. The second is the hot tide to use and exploit new energy worldwide which has taken the attention of geothermal scientists and engineers to high enthalpy geothermal resources in Tibet. The important scientific significance of geothermal research in Tibet is the third motivation. Tibet Plateau is said to be the third peak of the Earth. The historical and present processes in the plateau, its geology, geophysics and geochemistry, living, producing and physiological activities of local inhabitants, are all popular research topics in today's scientific field. The geothermal showing in the plateau is one of the most important links of scientific research. The geothermal systems all over the plateau are of great scientific importance and attract more and more scientists to set foot on the world peak. Many geologists would like to have an opportunity to explore the Tibet Plateau. The Yangbajing field is an ideal system to enhance the development of geoscience by geothermal research.

4.1.2 Geological tectonics of the field

The hot water in the bedrock and shallow reservoir includes three processes: recharge, horizontal flow and outflow:

1) *Recharge*, precipitation water percolates along fractures or pores to deep aquifers.
2) *Horizontal flow*, when the cold recharge has reached a certain depth, it tends to flow out horizontally while being heated by the anomalous high heat flow in the region (magmatic intrusion).
3) *Outflow*, the geothermal fluid rises along the fracture system because of its low density and high pressure and forms geothermal fields at a certain suitable geological structure.

The Yangbajing geothermal field is controlled by a crisscross of fault systems (Figure 10). The system consists of three N-E compresso-shear faults: (1) southern edge of Ningqingtangula Mountains, (2) China-Nepal Highway and (3) Changuoguo-Maluguo, and three perpendicularly N-W tenso-shear faults: (4) north of Qiangmaguo, (5) the Sulphur mine ZK-317 and (6) Thermal lake - Changuoguo. The faults (1), (3), (4) and (6) form the boundaries of the field (Kang et al., 1985).

FIGURE 10: Structural map of the Yangbajing system:

1. Quaternary system;
2. Triassic to Cretaceous system;
3. Granite from late Yanshan to Ximalaya;
4. Compresso-shear principal faults;
5. E - W regional compresso faults;
6. N-S faults;
7. Brush structure;
8. Occurrences of faults;
9. N-W tensile or tenso-shear faults;
10. Hot spring and its temperature (°C)

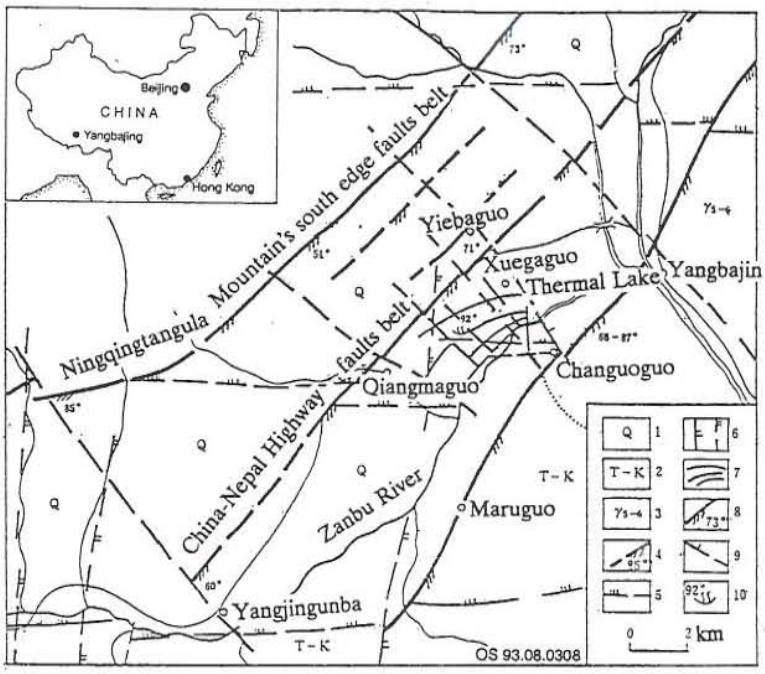

There is also a brush structure in the Yangbajing geothermal field located south of China-Nepal Highway, north to Zanbu River, west to Xuegaguo - Hot lake and east to Qiangmaguo-Zuoreguo. It diverges to the west and converges to the east. This brush structure is formed by the faults of China-Nepal Highway and Changuoguo-Maluguo. When the external part of the faults rotates counter clockwise relative to the inside, the converging part is twisted and ground pressure increased while the faults are being closed. On the other hand, the part from the middle to the diverging part is loosened and ground pressure decreased while the faults are being opened. The underground water flows from the converging to the diverging part. The orogenic cycle curvature at the middle part of the brush structure is the most productive with well developed tenso-shear fractures, which have high permeability and storativity.

There is dense and hard granite in the basement of Yangbajing. The tenso-shear faults formed by stress action are good flow paths for hot water to rise from the deep. The faults are very steep to control the vertical upflow of hot water in the basement and partly horizontal migration where the palingenetic fracture or pore system exists. This has been confirmed by the work to reveal the distribution of tritium (T) isotope in the field (Wei et al., 1983). The hot water flows up along the faults in the basement to the Quaternary grit layer to form a shallow reservoir. The faults extend deep in the reservoir according to the exploration data and there are also basement faults passing through the reservoir. The hot water not only migrates horizontally in the field, but also extends far away from the field boundary. It is certain that the hydrothermal activity is all over the Yangbajing Basin. The hot water flows to the boundary of the basin along the bottom of the Quaternary and the temperature and pressure decline gradually.

The hydrothermal alterations in the Yangbajing field are silification, kaolinization, alunitization and chloritization, which have a very clear horizontal distribution (Figure 11). The silification and alunitization are mostly near the faults but kaolinization is far from the faults.

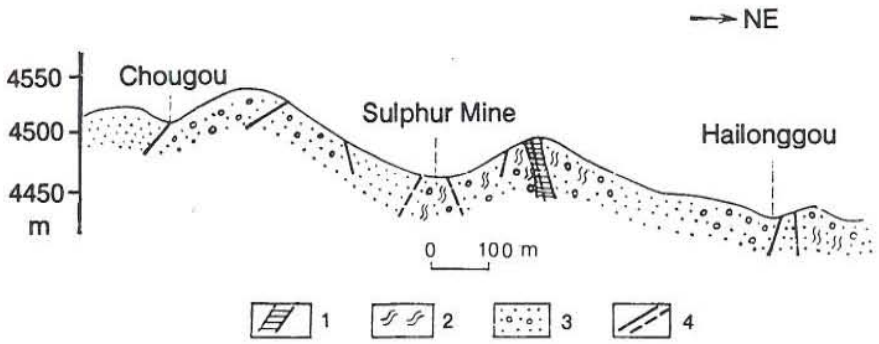

FIGURE 11: Hydrothermal alteration profile of the sulphur mine in the Yangbajing field: 1. Silification and alunitization; 2. Kaolinization; 3. Quaternary morainic layer; 4. Faults; (Kang et al., 1985)

The columnar section of the drilled wells shows the vertical distribution of the hydrothermal alteration with kaolinization on the top followed by poor kaolinization and silification. This is obviously controlled by the faults and hot water.

4.1.3 Geophysical survey in the field

The area of Yangbajing geothermal field is about 15 km^2 delineated by 30 Ωm contour of resistivity which coincides with 40°C temperature contour's delineation as mentioned before. The resistivity in the centre of the field is 4-5 Ωm, 20-30 Ωm at the boundary faults where it suddenly increases to several hundreds Ωm. This means the boundaries of the field are very clear. This may relate to the variation of lithofacies and be controlled by the faults. Figure 12 shows that the rock types of wells and the surface fluctuation of the reservoir basement are controlled by the granite.

The low permeability caprock of the reservoir is mostly clay in the southern part but morainal boulder clay in the northern part. The resistivity is only several of tens Ωm along the geophysical survey line 112 (Figure 13, see Figure 17 for location). This has a relation to the thickness of caprock, development of faults and their water contents. Also, the belt along line 112 has been proven to be the centre of the geothermal field.

The reservoir consists of Pleistocene sand, grit, sandstone and its hydrothermal precipitative cementation and sand. The granularity of the rock decreases from mainly sandstone in the northeast and northwest to grit and sand in the southeast and southwest. From the middle of the field, the thickness of the reservoir gradually decreases toward the northwest and southeast but increases toward northeast and southwest.

The fissure bedrock reservoir lies north to the highway of China-Nepal and connects with the top Quaternary sedimentation to form a united hydrothermal system with no aquiclude between them. The basement of the reservoir is mostly granite which is overlaid by a thin tuff layer in the southern part of the field. Therefore, the whole Quaternary reservoir has good water convection with caprock in the south but none in the north.

The borehole temperature gradient, especially in wells ZK-318, 203, 403, 319 and 313 in Figure 14, shows that there is a lateral migration in the shallow reservoir and that the temperature of the borehole decreases with depth when it is in the bed rock.

Generally, convection occurs at above 800 m depth while conduction happens in the underlying basement. What people are most interested in is whether there is another deep reservoir with higher temperature and pressure. In the deepest well, ZK-308, the granite extends to a depth of 1700 m, which has the same age as the granite in the basin's two sides as determined by isotopic age method.

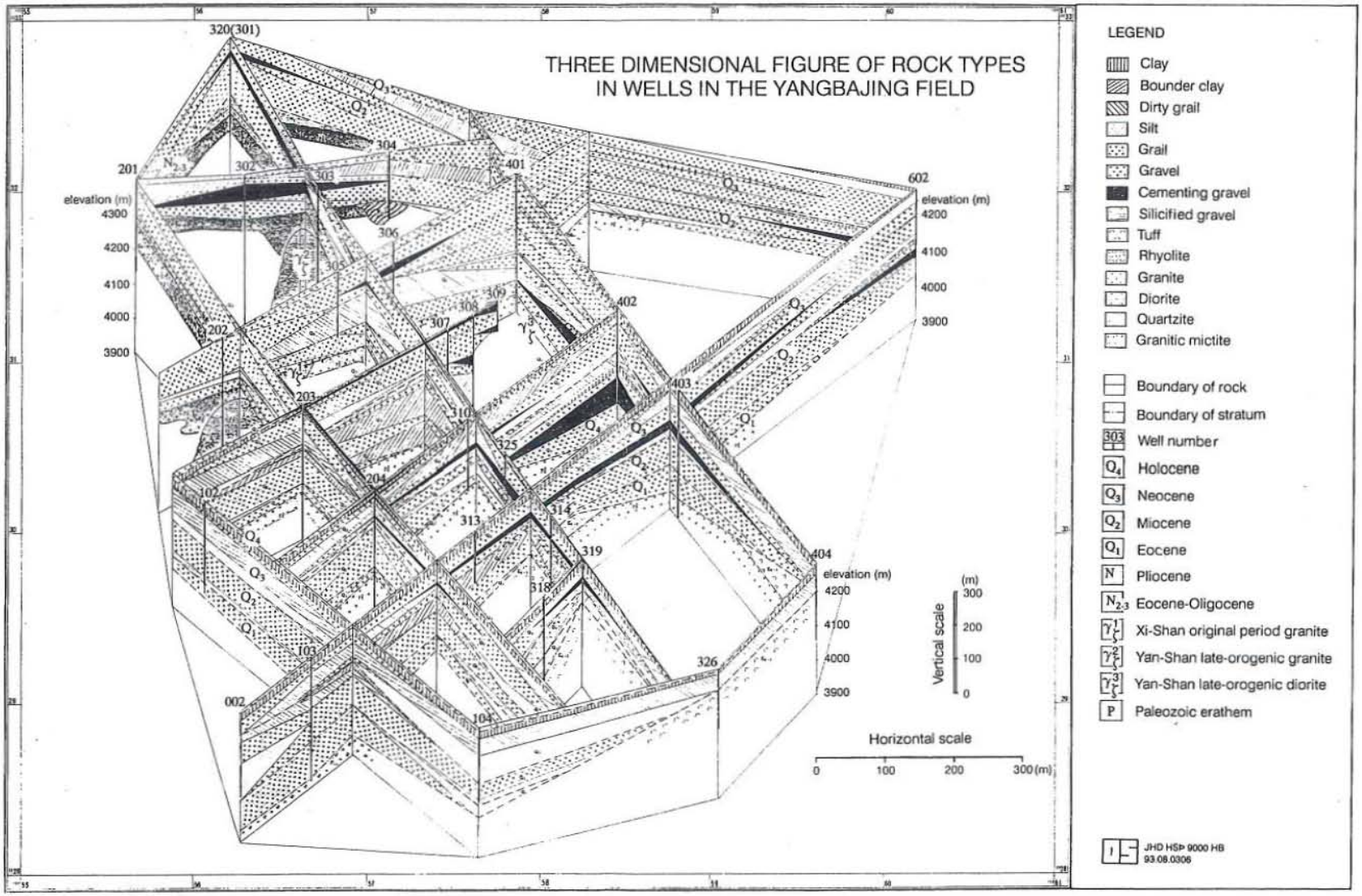

FIGURE 12: Three dimensional figure of rock types in the wells in the Yangbajing field

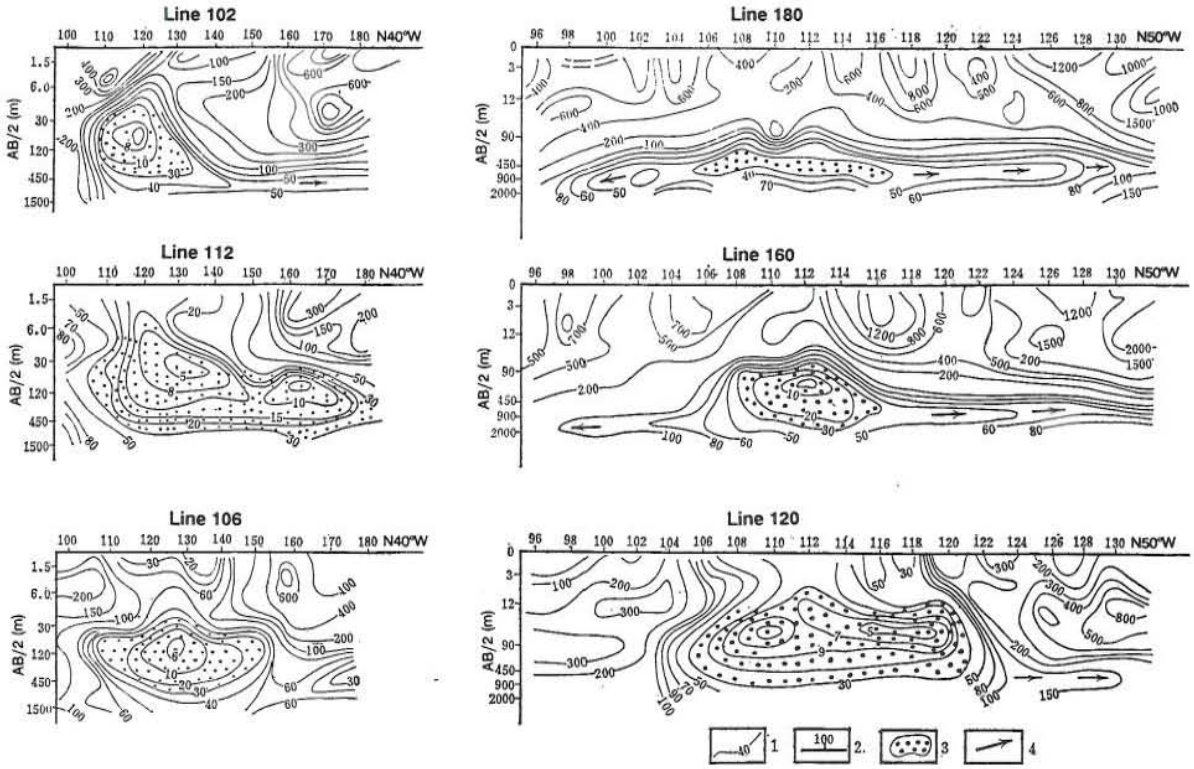

FIGURE 13: Isolines of apparent resistivity ρ_s, along geophysical survey lines 102, 112, 106, 120, 160, 180 in the Yangbajing field; 1. Isoline of ρ_s (Ωm); 2. Survey point number; 3. Reservoir; 4. Direction of flowing hot water (Kang et al., 1985)

It infers that all the granite in this area is connected and extends very deep. The reservoir is liquid-dominated, however, boiling was usually observed in the flowing wells at 10-50 m from the surface. The water boils at 86.5°C because of the local low atmosphere pressure. Figures 15 and 16 show the temperature and pressure contours at 20 m depth below surface in the field.

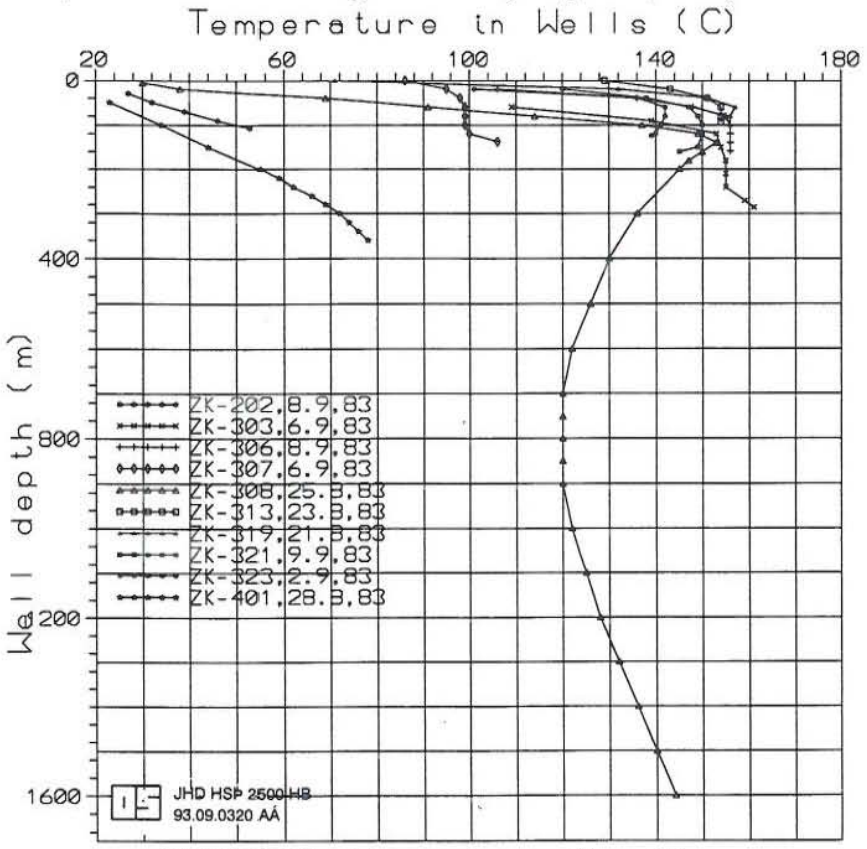

FIGURE 14: Temperature profiles of the wells in the Yangbajing field

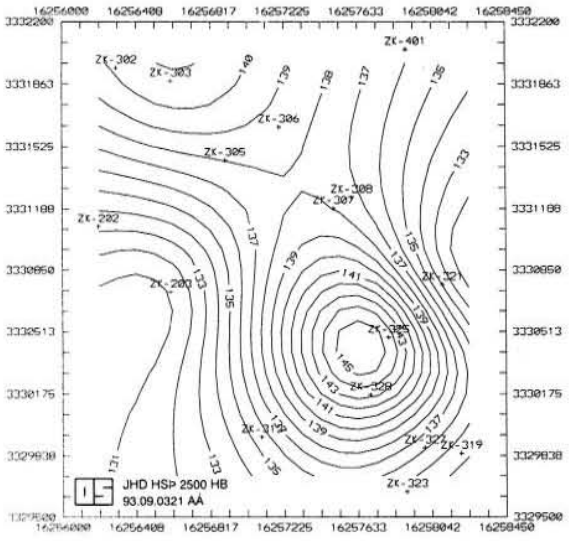

FIGURE 15: Temperature contours (°C) of the wells at Z=20 m below surface

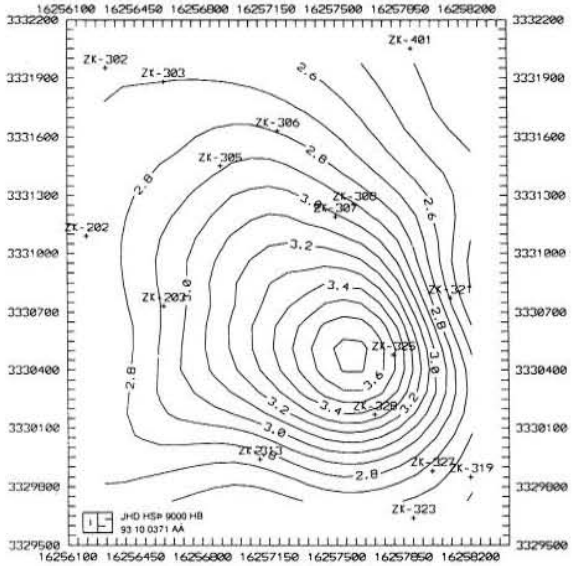

FIGURE 16: Pressure contours (bar) of the wells at Z=20 m below surface

4.1.4 Geochemical survey in the field

The hydrochemical water types in the field are mostly Cl-Na, HCO_3-Cl-Na and a little SO_4-Na. The Cl-Na waters have slightly higher temperatures in a borehole than in hot springs.

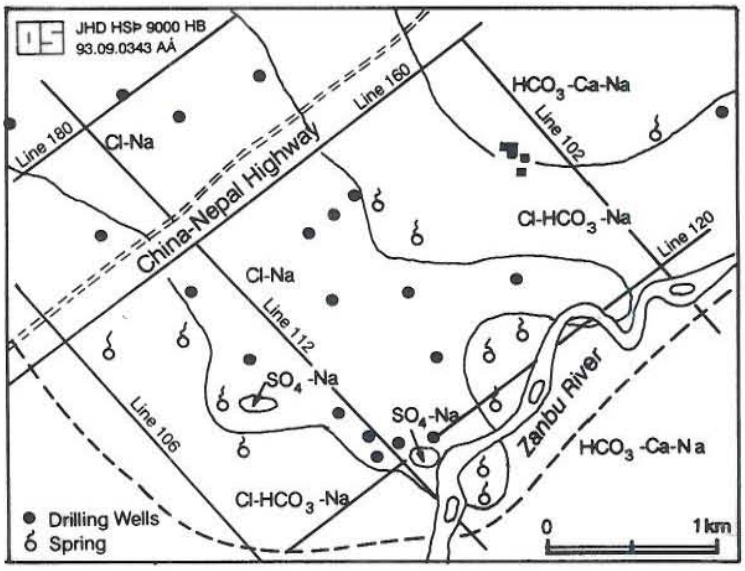

FIGURE 17: Distribution of hydrochemical types in the Yangbajing field (Kang et al., 1985)

The HCO_3-Cl-Na water means that the water in the reservoir has been mixed with cold surface water. The SO_4-Na type is only found in the "92°C Spring" area, wherein the H_2S in the hot water is oxidized into sulphuric acid.

Figure 17 shows a regular distribution from the centre (Cl-Na) to the boundary of the field (HCO_3-Cl-Na), and the inferred flowing paths and temperature of water. The pH value of the hot water is about 7-8. The gases in the water are mostly CO_2 (>80%) and a little H_2S, H_2, N_2 and CH_4.

Table 1 shows that the δD in hot water ranges from -150 to -160 and that $\delta^{18}O$ is between -17 and -20. This is different from δD (from -40 to -80) and $\delta^{18}O$ (from 6 to 9) found in magmatic water but similar to that of precipitation water in the Yangbajing area. This means that the main source of hot water is precipitation.

TABLE 1: Isotopic composition of hot and surface water in the Yangbajing field (Wei et al., 1983)

Well No.		309	316	315	312	204	314	310	317	313
M. data	δD	-143.2	-146.0	-147.3	-147.3	-147.8	-148.0	-148.6	-150.7	-149.3
	δ^{18}O	-15.66	-16.11	-17.74	-17.82	-17.80	-17.95	-18.46	-18.21	-18.76
	T	<1	<1	3.3	7.5	8.4	<1	<1	7.0	7.0
C. data	δD	-150.1	-149.8	-153.5	-153.9	-153.9	-154.1	-153.0	-155.0	-156.1
	δ^{18}O	-17.07	-16.87	-19.00	-19.15	-19.02	-19.20	-19.35	-19.06	-20.13

Well No.		302	307	311	303	319	403	203	IS-1	W-24
M. data	δD	-150.0	-150.3	-151.0	-151.8	-153.2	-153.6	-154.8	glacier	Z.B.
	δ^{18}O	-18.23	-18.70	-18.68	-18.38	-18.44	-19.20	-19.35	ice	river
	T	8.2	18.9	8.9	2.5	<1	2.9	3.2		water
C. data	δD	-157.1	-157.2	-157.9	-158.8	-160.3	158.9	-159.8	-174.5	-141.0
	δ^{18}O	-19.65	-20.10	-20.08	-19.80	-19.88	-20.27	-20.36	-23.38	-19.89

M. data - Measured data; C. data - Calibrated data after steam and water separation.
Remarks: The last two are surface water samples, one came from glacier ice northwest of the basin and the other one from Zanbu River.

Tritium is a radioactive hydrogen isotope whose period of half decay is 12.3 years. Usually, there is no tritium in geothermal water due to its long distance migration, however, tritium is high in precipitation water. Therefore, if the geothermal water is mixed with cold surface water, tritium may be found in it.

As shown in Table 1, wells in the central area (such as ZK-309, 316, 314, 310 and 319) have very low concentration of tritium (<1) while the outside wells have relatively high concentration of tritium because of cold water mixture. This states clearly that the hot water in the central area flows up directly from vertical fractures in the basement or migrates horizontally from the north part.

There is an "O-18 shift" in Figure 18, which means that the Yangbajing field is a high temperature hydrothermal system. The concentrations of fluorine (F^-) and silica (SiO_2) in the hot water are very high, the concentration of F^- is about 5-15 mg/l while the concentration of SiO_2 is about 100-200 mg/l. The concentration of HBO_2 in the water is also very high (100-200 mg/l) and is directly proportional to the concentration of Cl in the water (Figure 19).

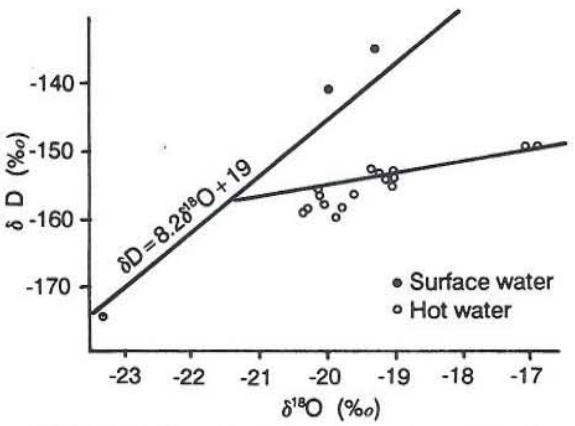

FIGURE 18: Relation between δD and δ^{18}O in hot and surface water (Kang et al., 1985)

Figure 20 shows the regular decline of concentration of fluorine and silica, which relates the heat anomaly centre and main paths of upflowing water. The study of chemical contents of geothermal hot water is very important not only for the originality of the field, water source and temperature at depth, but also to delineate the centre of the thermal anomaly and the paths of hot water.

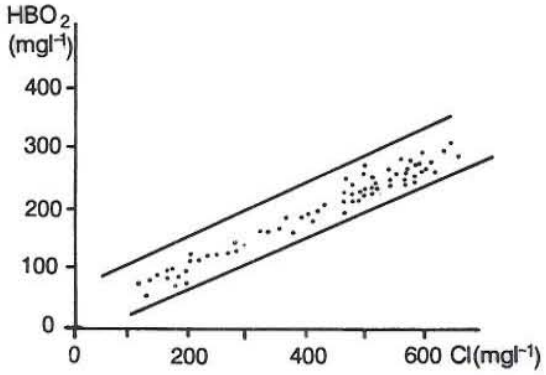

FIGURE 19: Relation between HBO_2 and Cl in the Yangbajing field (Kang et al., 1985)

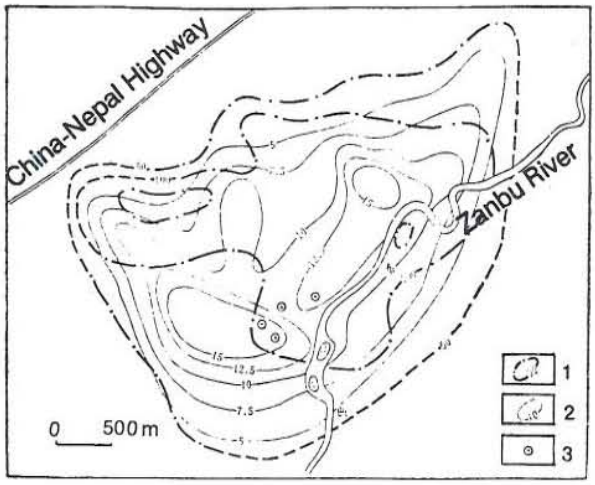

FIGURE 20: Isoline of silicic acid and fluorine ion in the Yangbajing field: 1. H_2SiO_3 (mg/l); 2. F^-(mg/l); 3. Borehole; (Kang et al., 1985)

All kinds of data state that the centre belt of the heat anomaly in the field is along the range of wells ZK-304, 302, 303, 309, 310, 311, 322 and 316. This has been commonly accepted. However, where the main flow paths for hot water in this belt are, is still open for speculation.

In general, there are two main theories. One theory says that the hot water flow paths are located in the northern part of the field, especially in the area of the "Sulphur mine". The hot water flows up to the shallow ground along the cracks then migrates to the southeast of the field. The Cl-HCO_3-Na type water in the shallow reservoir was considered to be just a mixture of Cl-Na type and HCO_3-Ca-Na type water in the deep of the reservoir (Liao and Wu, 1985). Another person who also held this opinion states that the source of heat and water is in the north of the field and that a northwest tenso-shear fault is the main flow path for hot water (Yao et al., 1985). After mixing with precipitation and melted snow, the field fluid flows to the south of the field and manifests as surface springs.

The other theory supposes that there are hot water flow paths in the northern part (near wells ZK-304, 302 and 303) and in the southern part (near wells ZK-309, 310, 311, 322 and 316) separately (Kang et al., 1985). There are three main agreements for this:

1) Most of the main faults of the field are located in the south. According to the physical exploration, there are two main fracture zones in the field: the northeast compresso-shear and northwest tenso-shear fractures. The crisscross of these two main fracture zones are all possible flow paths for hot water. This is consistent with the anomalous heat belt along the northwest geophysical survey line 112. All the researches (from 1984 to 1985) state that flow paths for hot water should be located at the secondary fractures not the primary ones. Thus, the main fault just before the Ningqingtangula mountains should not be the main flow path for the hot water.
2) The centre of low resistivity is in the south and gradually increases in an outward direction. This distribution should be regarded as an expression of hot water flow paths.
3) The good reservoir parameters are all in the south. Wells ZK-309, 311 and 322 in the south have high temperature, pressure and flowrate. If the hot water came from the north, all geothermal parameters would obviously decline, especially in wells ZK-316 and 318 which are far from the north.

Shen (1984) presented a hydrothermal model with different flow paths of hot water recharge in the northern and southern parts. The northern part of the reservoir is possibly open to some hot liquid from deep magma. This is the reason that the temperature in the northern basement may be as high as 200-220°C. The hot water supply in the north is mixed with the cold water from the Ningqingtangula mountains. The mixed fluid migrates from the N-W to the E-S part of the field driven by gravity. The distribution and storage range of hot water is determined not only by the distribution of reservoir permeability but also by the dynamic balance with the cold water pressure at its two sides. In the southern part of the reservoir, the hot fluid heated during a deep circulation may have a near surface mixing with cold water when it flows up along the faults. This "primary mixing" causes the water temperature to drop 10°C less than that in the northern part, which is usually about 165°C. According to the distribution of temperature and pressure, the hot fluid supply area should be located in the middle of the southern part of the field which is north to the Zanbu river.

It is still very difficult to say which is the best model for the field. The deep-going exploitation and exploration work will be carried out in the following years. There is still very urgent reservoir engineering work to be done in the Yangbajing geothermal field.

4.1.5 Drilling and production history

Much of the exploration work in the field has been carried out during the last two decades and the field has been under exploitation since 1976. In the past sixteen years, the work on geology, well drilling, geophysical and chemical exploration has all been carried out simultaneously with the collecting of data from more than forty exploration and production wells. The first 100 kW pilot geothermal plant was built in 1977. It did not only change the energy composition in Tibet, but also opened a new page for the research work of new energy and renewable energy in China. In 1985, the Yangbajing field produced 20 MW_e from its geothermal resources. This was equivalent to about 80% of the geothermally generated electricity in China and was 21% of Tibet's energy consumption. Table 2 gives general information on all the drilled wells in the Yangbajing field. Table 3 shows the parameters of producing wells and their potential power capacity.

4.2 Basic assumptions and initial parameters for the model

Drilling and geological exploration have shown that the Quaternary morainal grail layer in the Yangbajing field has very good permeability. However, it is anisotropic in both the vertical and horizontal directions. The dense and hard granite in the bedrock has very low permeability because of poor porosity and fracture development. Therefore, the high permeable zone in the bedrock must be connected with the main hot water transportation paths. All the wells have different temperature, pressure and permeability (Table 4).

The total surface area covered by the calculation mesh is about 118 km^2. The model was created with 521 nodes and 764 elements. The northern boundary conditions for the distributed model are established as fixed source flow boundaries because of the recharge from the northern mountains. The other boundaries are all set at no-flow. As to the initial state prior to production, it was assumed that the reservoir water head was constant so that there was no hydraulic gradient in the area at the beginning.

TABLE 2: General information on all the wells in the Yangbajing field

Well no.	Drilling time	Well type	Elevation (m a.s.l.)	Well depth (m)	Casing depth (m)	Remarks
ZK002	84.6.23-7.21	e	4286.1	261	68	
ZK102	84.5.13-6.4	e	4290.9	274	19	
ZK103	83.5.26-7.19	e	4284.5	366	87	
ZK104	84.8.5-9.8	e	4280.8	251	43	
ZK201	81.5.24-11.3	e	4404.5	269	96	
ZK202	81.5.7-7.20	e	4316.0	357	196	
ZK203	77.10.17-12.1	e&p	4297.2	457	255	good
ZK204	80.4.7-5.22	e&p	4287.1	551	235	good
ZK301	82.6.12-6.22	e	4427.2	240	179	abandoned
ZK302	79.4.8-6.10	p	4352.9	457	288	excellent
ZK303	79.7.9-7.31	e&p	4332.8	336	268	excellent
ZK304	78.8.14-10.13	e&p	4333.6	206	126	good
ZK305	79.5.-	p	4315.3	203	202	good
ZK306	79.9.7-9.25	p	4310.3	223	219	good
ZK307	79.8.29-9.24	p	4298.1	341	241	good
ZK308	82.6.5-10.23	e	4297.3	1726	483	
ZK309	78.5.23-6.23	e&p	4298.0	87	65	excellent
ZK310	79.6.14-7.3	p	4290.6	213	171	good
ZK311	80.6.26-7.18	p	4286.3	81	57	excellent
ZK312	80.7.26-8.21	p	4283.3	225	160	good
ZK313	78.8.4-8.27	p	4283.2	155	149	excellent
ZK314	78.9.30-11.19	e&p	4284.0	354	236	good
ZK315	77.8.20-9.19	p	4281.7	68	68	excellent
ZK316	75.7.1-9.2	e	4283.1	42	37	abandoned
ZK317	76.8.30-9.	e	4284.7	64	36	abandoned
ZK318	77.7.10-8.13	p	4283.7	311	299	good
ZK319	80.6.1-6.23	p	4284.5	156	126	excellent
ZK320	82.8.1-10.21	e	4427.2	252	173	
ZK321	82.5.21-6.28	p	4286.6	179	115	
ZK322	82.7.4-8.6	p	4283.0	107	74	abandoned
ZK323	82.8.20-9.19	p	4281.1	131	135	
ZK324	82.9.27-10.21	p	4289.9	90	81	
ZK325	84.7.18-8.5	p	4285.6	94	70	
ZK326	84.8.23-9.17	e	4281.1	172	0	
ZK327	84.5.27-6.15	p	4282.2	118	118	
ZK328	84.6.23-7.10	p	4284.0	108	108	
ZK401	83.5.29-8.3	e	4308.3	453	40	
ZK402	84.5.22-7.9	e	4286.3	263	81	
ZK403	78.6.28-8.20	e&p	4279.7	603	276	
ZK404	84.7.19-8.14	e	4282.4	221	92	
ZK602	78.10-3-12.9	e	4285.0	185	-	abandoned

e - exploratory well; e&p - exploratory and producing well; p - producing well;

TABLE 3: Parameters of wells in the Yangbajing field

Well no.	Max.T in well (°C)	Work T at wellhead (°C)	Work P at wellhead (bar)	Lip P (bar)	Total flow (kg/s)	Steam flow (kg/s)	Steamr atio (%)	Power potential (kW)*
ZK203	141	125	2.3	0.766	23.8	2.5	10.73	818.5
ZK204	147	122	2.3	0.716	21.2	2.5	11.95	767.3
ZK302	172	137	3.6	1.066	25.7	4.4	17.23	1124.2
ZK303	167	134	3.2	1.066	26.9	4.3	15.70	1109.9
ZK304	172	133	3.8	1.066	25.7	4.5	12.24	1109.9
ZK309	160	146	4.6	1.916	49.0	7.2	14.63	1948.8
ZK310	160	125	2.9	0.836	22.4	3.3	14.63	890.2
ZK311	157	147	4.7	1.716	45.6	6.4	14.00	1775.6
ZK312	149	138	3.7	1.116	32.0	4.0	12.36	1174.8
ZK313	161	131	3.3	0.966	25.2	3.7	14.85	1009.8
ZK314	160	131	3.5	1.106	28.9	4.4	15.09	1164.7
ZK315	152	127	3.1	1.856	20.1	2.7	13.17	761.2
ZK319	161	130	3.3	1.116	29.3	4.4	14.84	1174.8
ZK321	155	120	2.1	0.716	20.0	2.7	13.61	767.3
ZK324	160	147	4.3	1.816	47.1	6.9	14.66	1874.8
ZK325	155	143	4.1	1.666	45.0	5.6	13.60	1725.9
ZK327	152	116	2.6	0.916	25.9	3.4	12.98	971.9
ZK328	152	138	3.5	1.370	38.1	4.8	12.98	1430.4

* The reference temperature for the calculation is 85°C.

TABLE 4: Reservoir parameters from well testing in the Yangbajing field

Method	Main well	Observ-ation well	Pressure data	Analysis method	Calculation results	
					$T(m^2/s)$	$S*10^{-6}$
Multiple & lip	ZK314	ZK310 ZK315	pressure drawdown	ΔP-lgt	.02131	58.9
	ZK312	ZK319 ZK314 ZK310			.06376	2066
	ZK313	ZK315			.01759	177
	ZK309	ZK310 ZK304	waterlevel drawdown	S-lgt	.12354	33.0
	ZK319	ZK314	pressure drawdown	ΔP-lgt	.17395	44.6
Single & lip	ZK321				.01444	
Average					.06910	476.2
Interference & lip	ZK303 ZK302 ZK304	ZK305	waterlevel drawdown& build-up	S-lgt S-lg(1+ t_p/t')	.03694 .05855	235.6
Multiple & lip	ZK302	ZK303	waterlevel drawdown	S-lgt	.12862	48.1
	ZK303	ZK302 ZK306	waterlevel build-up drawdown	S-lg(1+ t_p/t') S-lgt	.04394 .08907	81.8 50.0
Average					.06642	92.1

4.3 Results from the calibration

The transmissivity in the area covered by the model varies from 5.00×10^{-4} to 7.5×10^{-2} m^2/s (Figure 21). The lowest value covers the outside of the production zone in the Yangbajing Basin while the transmissivity in the reservoir is very high. The storage coefficient distribution for this model varies from 8.0×10^{-4} to 0.17 (Figure 22).

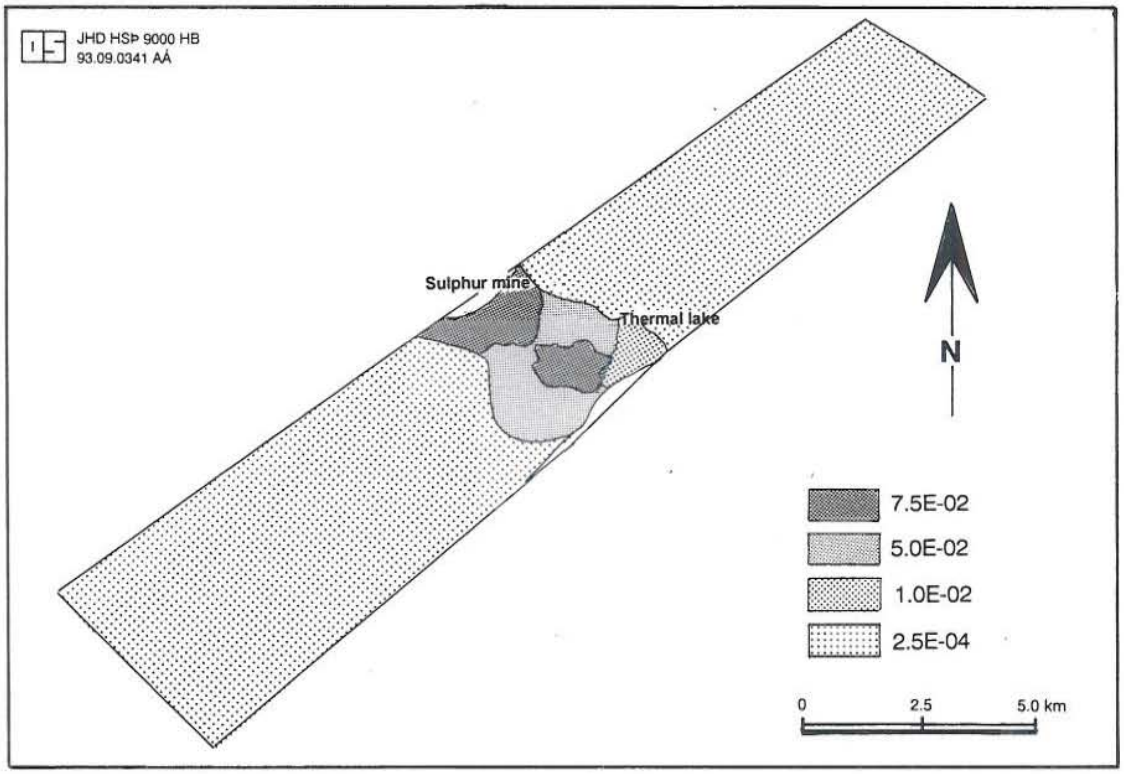

FIGURE 21: Transmissivity (m^2/s) distribution in the Yangbajing field

The highest value is assigned to the two-phase zone in the northern part of the field. This obtained value is very high if it is compared with the values calculated by well testing. It is possible to explain with two different storage mechanisms which appear during the exploitation of the field because the dry steam storativity is much greater than the compressible storativity of a liquid-dominated reservoir. During utilization of the reservoir, the increase of the storativity is mainly due to delayed yield and double porosity effects (Figure 23).

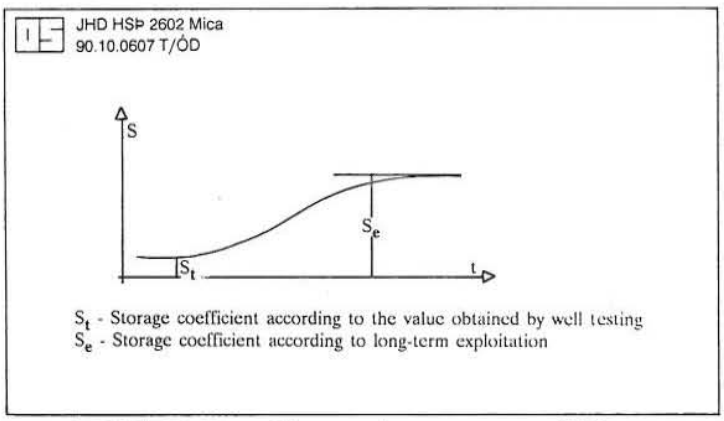

FIGURE 23: Changes in storage coefficient during exploitation (Martinovic, 1990)

The distribution of anisotropy angle in the Yangbajing field is shown in Figure 24. The longitudinal transmissivity (T_{xx}) and transverse transmissivity (T_{yy}) ratio (sqrt(T_{yy}/T_{xx})) are set at 0.477 in the southern part, 0.316 in the northern part of the producing area and 0.8 outside. The values are taken from the geological survey in the field.

The calculated water level for well ZK-306 under different production rates is shown in Figure 25.

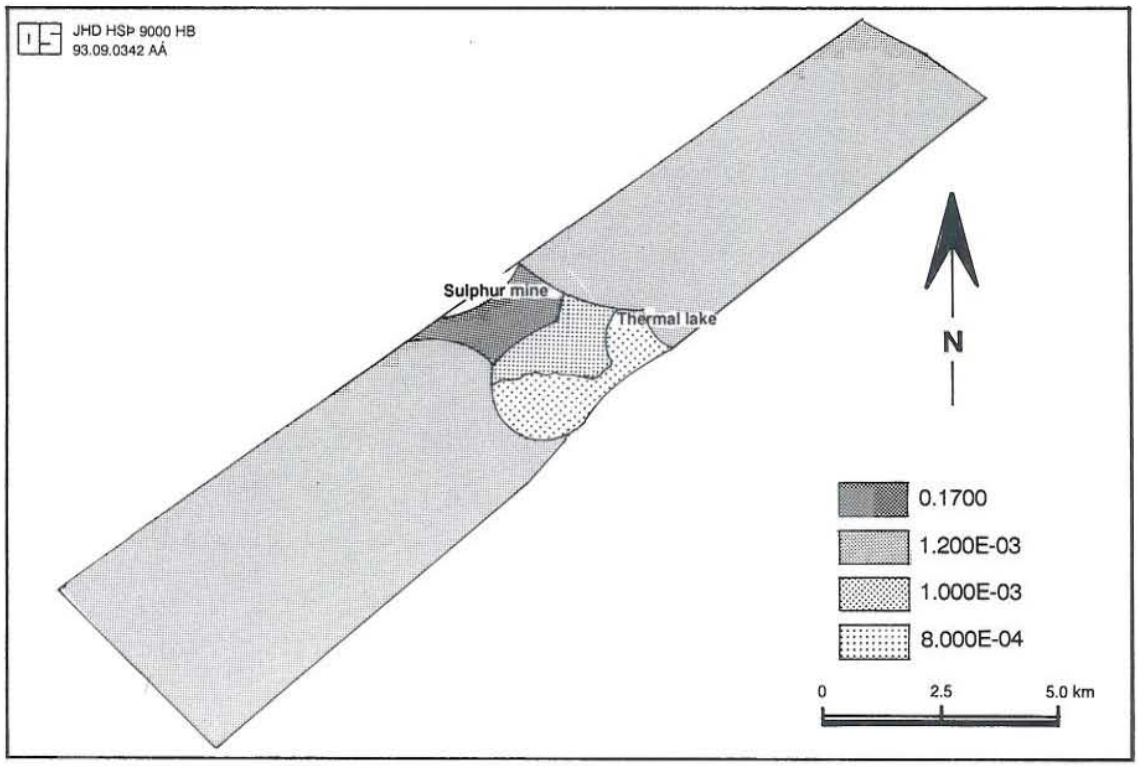

FIGURE 22: Storativity distribution in the Yangbajing field

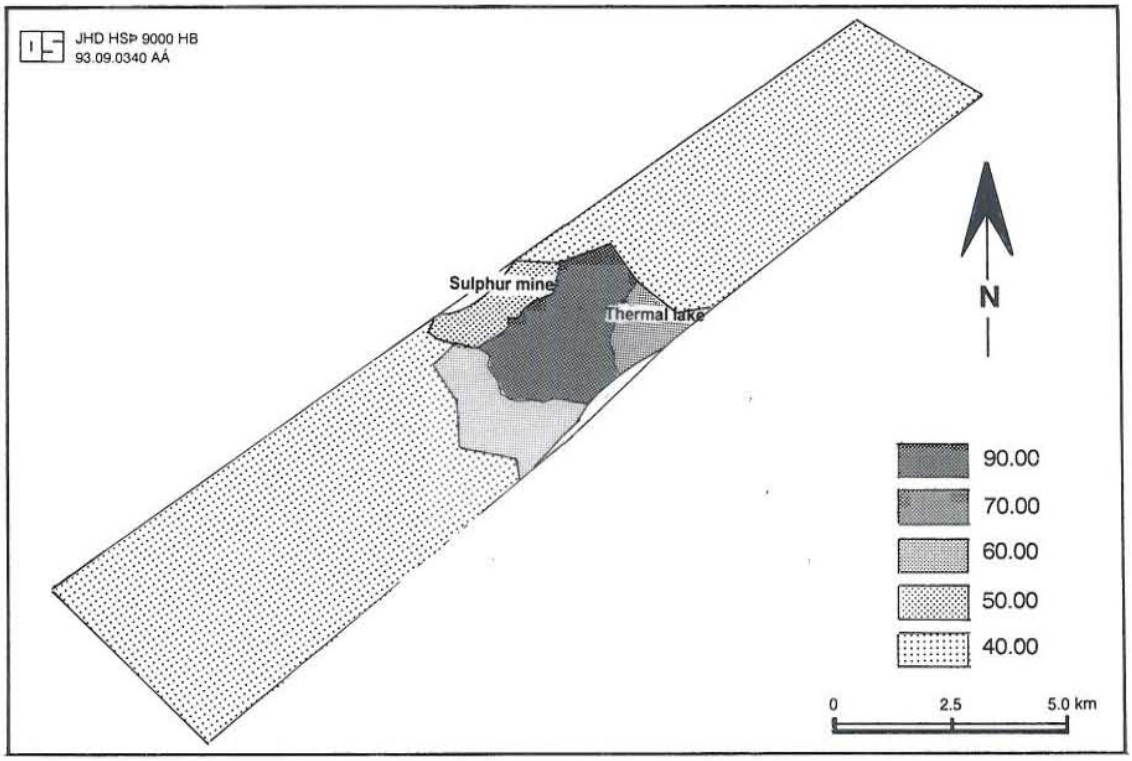

FIGURE 24: Anisotropy angle distribution in the Yangbajing field

When the production was increased from 200 kg/s to 550 kg/s, water level drawdown increased rapidly in the reservoir. Therefore, the reinjection rate of 170 kg/s is taken into account in the future prediction in the Yangbajing field. The reinjection is supposed to be carried out in two ways.

The first scheme is to put the reinjection wells in the northern part to mix with the recharge water in the vertical convection before the water enters the reservoir at 140°C.

The other strategy is to put the reinjection wells in the southern part close to the power plant and to use 80°C waste water from the plant. The temperature decline due to cold water reinjection is shown in Figures 26 and 27

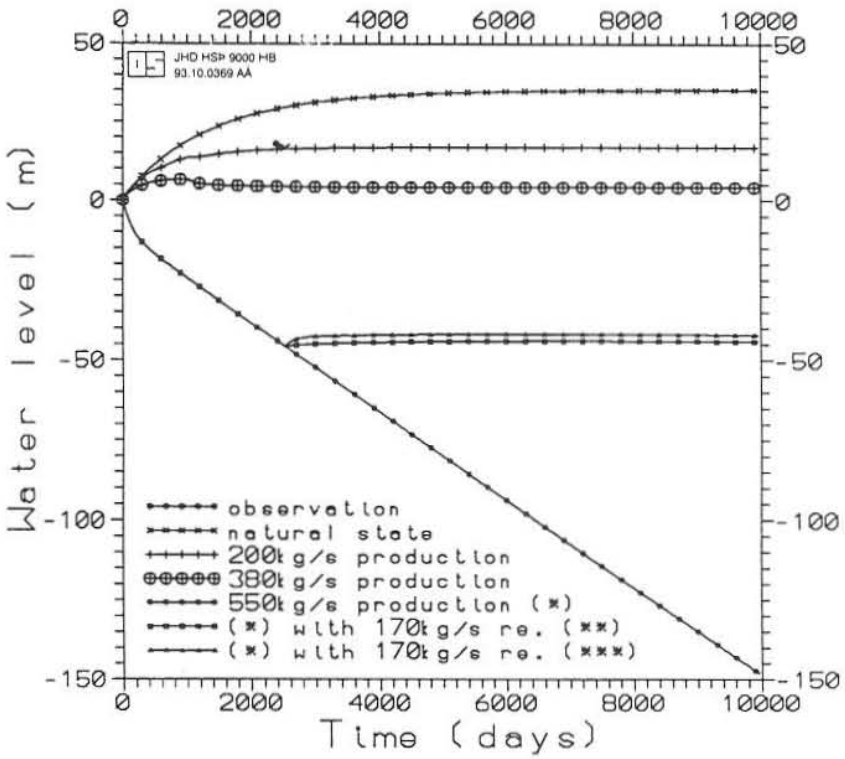

FIGURE 25: Water level under different production rates and reinjection

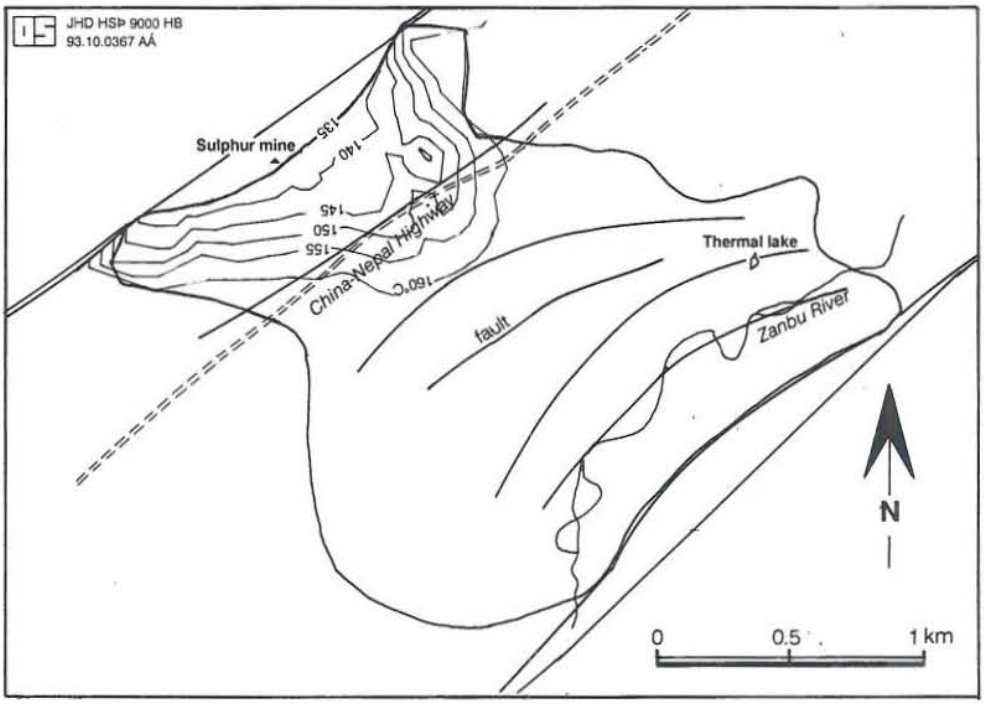

FIGURE 26: Temperature decline with reinjection in northern Yangbajing field

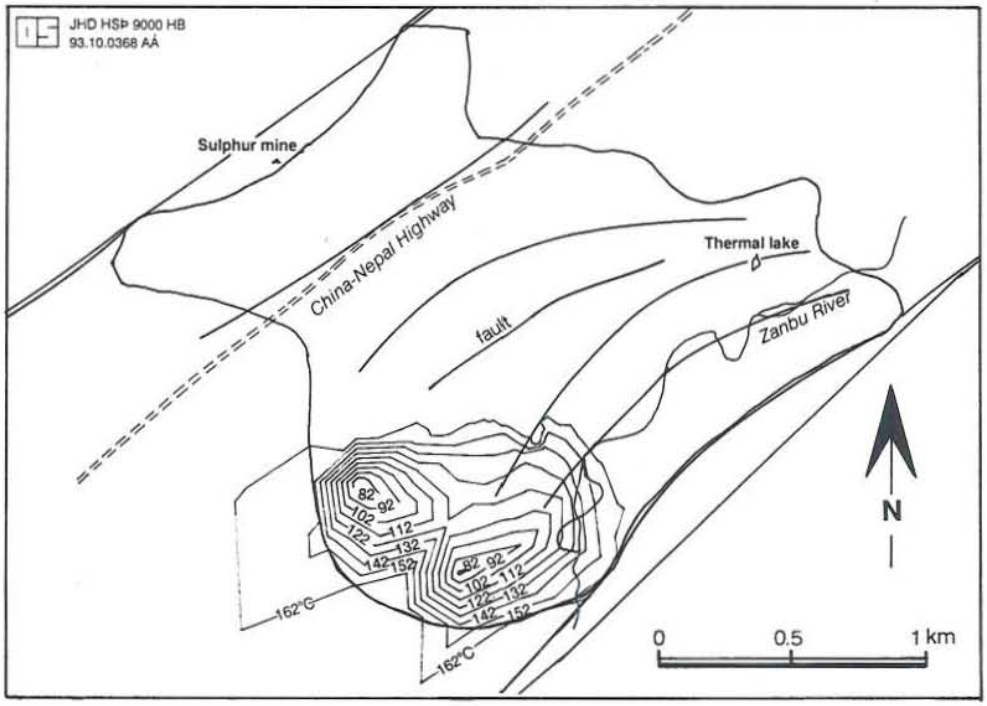

FIGURE 27: Temperature decline with reinjection in southern Yangbajing field

The parameters used for the heat transport problem are as follows:

Longitudinal dispersity:	50 m;
The ratio of sqrt(α_T/α_L):	0.316;
Porosity of the reservoir:	0.17;
Retardation constant:	0.238;
Aquifer thickness:	200 m;
Initial temperature:	165°C;
Decay constant (S^{-1}):	0;
Molecular diffusion (D_m, L^2/s):	0;
Upstream weighting factor (μ, 0-1):	0;
Value of "n" in "$\phi D_{xx}=a_L v^n+D_m\phi$" (>0):	1.

The results above were obtained with the assumption that there is an upflow of hot water from the basement in both the southern and northern parts. If there is only a channel for hot water in the northern part, the transmissivity parameter for the model is two times the former one in order to fit the observation data in well ZK-306. This parameter is rather high.

4.4 Conclusions and recommendations

The simulations under different assumptions for hot water upflow from the basement show that the theory which assumes the upflow in both parts of the field is more reasonable. The study of the Yangbajing geothermal field also shows that if the production rate is greater than the recharge of the field, the water level in the field will be drawn down very fast. Reinjection can be effective to maintain the water level in the field.

Reinjecting water at 80°C, either in the north or south, would not drastically cool down the reservoir. Although the distributed parameter model is already capable of predicting the future responses of the field, its accuracy can further be enhanced by a re-evaluation using more time-dependent production and observation data.

ACKNOWLEDGEMENTS

I would like to leave my thanks here, and take your kindness and experience with me back to my home:

- to Dr. Ingvar Birgir Fridleifsson, the director of the UNU Geothermal Training Programme, for granting me the opportunity to attend the UNU geothermal course and providing excellent work conditions during my entire study;

- to my supervisor, Dr. Snorri Pall Kjaran, for his guidance during the specialized reservoir engineering course;

- to Mr. Ludvik S. Georgsson and Mr. Sigurdur Larus Holm for their patient and detailed assistance;

- to the lecturers for their comprehensive presentations, especially to Benedikt Steingrimsson, Grimur Bjornsson, Gudni Axelsson, Thordur Arason, Valgardur Stefansson, Omar Sigurdsson and Hilmar Sigvaldason for their willingness to share their knowledge and experience; and

- to Ms. Margret Westlund and Ms. Chona C. Bustamante for correcting my report, Ingibjorg Gisladottir and Erla Sigthorsdottir in the library, Audur Agustsdottir and Helga Sveinbjornsdottir in the drawing room for their kind help.

Finally, I would also like to extend my gratitude to Tsinghua University and my supervisors, Prof. Wang Buxuan, Prof. Lu Run and Prof. Shen Xianjie for their support during my studies in China.

NOMENCLATURE

a_L - longitudinal dispersity [m]
a_T - transversal dispersity [m]
b - aquifer thickness [m]
c - solute concentration [kg/m^3]
c_o - solute concentration of vertical inflow [kg/m^3]
c_w - solute concentration of injected water [kg/m^3]
C_l - specific heat capacity of the liquid [kJ/kg°C]
C_s - specific heat capacity of the porous media [kJ/kg°C]
D_m - molecular diffusivity [m^2/s]
D_{xx} - dispersion coefficient in x direction
D_{yy} - dispersion coefficient in y direction
h - groundwater head [m]
h_o - head in upper aquifer [m]
k - permeability of semipermeable layer [m/s]
K_d - distribution coefficient
m - aquitard thickness [m]
R - infiltration [mm/year]
R_d - retardation coefficient
S - storage coefficient
t - time [s]
T - temperature [°C]
T_o - temperature in vertical inflow [°C]
T_{xx} - transmissivity in x direction [m^2/s]
T_{yy} - transmissivity in y direction [m^2/s]
Q - pumping/injection rate [m^3/s]

Greek symbols:

β_c - retardation constant [mass transport]
β_h - retardation constant [heat transport]
∂_l - density of the liquid [kg/m^3]
∂_s - density of the porous media [kg/m^3]
ϕ - porosityγ - leakage [m/s]
κ - time constant [s]
λ - decay constant [s^{-1}]
ν - velocity [m/s]
ν_x - velocity vector [m/s]
ν_y - velocity vector [m/s]

REFERENCES

Bjornsson, G., and Steingrimsson, B., 1992: Fifteen years of temperature and pressure monitoring in the Svartsengi high-temperature geothermal field in SW-Iceland. Geothermal Resources Council, Transactions, 20, 627-633.

Bodvarsson, G.S., Pruess, K., and Lippman, M.J., 1986: Modelling of geothermal systems. J. Pet. Tech. Sept., 1986, 1007-1021.

ENEL-AQUATER (ENI), 1985: Reservoir and production engineering study of the Yangbajing geothermal field in Tibet. Draft final report, Annex 5.

Franzson, H., 1983: The Svartsengi high-temperature field, Iceland, subsurface geology and alteration. Geothermal Resources Council, Transactions, 7, 141-145.

Georgsson, L.S., 1984: Resistivity and temperature distribution of the outer Reykjanes Peninsula, Southwest Iceland. 54th Annual international SEG Meeting, Atlanta, Ga., Extended Abstracts, 81-84.

Kang Wenhua, Li Delu, and Bai Jiaqi, 1985: Geothermal geology of the Yangbajing geothermal field in Tibet. Bulletin of the Institute of Geomechanics, CAGS (in Chinese), 6, 7-71.

Liao Zhijie, and Wu Fangzhi, 1985: The structure model on the Yangbajing field, Research on the Yangbajing geothermal power station (in Chinese). In Liu Diangun (ed.): Research on the Yangbajing Geothermal Power Station, Publishing House Chongqing Branch for Scientific and Technical Documents, 136-147.

Martinovic, M., 1990: Lumped and distributed parameter models of te Mosfellssveit geothermal field, SW-Iceland. UNU G.T.P., Iceland, report 9, 37 pp.

Palmason, G., and Gudmundsson, A., 1990: Iceland country update. Geothermal Resources Council, Transactions, 14-1, 111-126.

Shen Xianjie, 1984: The analysis of the reservoir structure model for the Yangbajing geothermal field. Chinese Science (in Chinese), 10, 941-949.

Vatnaskil Consulting Engineers, 1990: AQUA, user's manual. Vatnaskil, Reykjavik.

Wei Keqin, Lin Ruifeng, and Wang Zhiqiang, 1983: Isotopic composition of H, O and Tritium in the hot water in the Yangbajing field, Tibet. Geochemistry (in Chinese), 4, 338-345.

Yao Zhujin, An Keshi, and Zheng Zhouhua, 1986: An assessment of geothermal resources in Yangbajing, Tibet. Bull. Institute of Hydrogeology and Engineering Geology, CAGS (in Chinese), 2, 1-52.